Energy conversion by parallel electric fields during guide field reconnection in scaled laboratory and space experiments

W. Fox[1,2], F. D. Wilder[3], S. Eriksson[3], J. Jara-Almonte[1], F. Pucci[1,4], J. Yoo[1], H. Ji[1,2], M. Yamada[1], R. E. Ergun[3], M. Oieroset[5], and T. D. Phan[4]

[1]Princeton Plasma Physics Laboratory, Princeton, NJ 08543
[2]Department of Astrophysical Sciences, Princeton University, Princeton, NJ 08544
[3]Laboratory for Atmospheric and Space Physics, University of Colorado Boulder, Boulder, Colorado, USA
[4]National Institute for Fusion Science, National Institutes of Natural Sciences, Toki 509-5292, Japan
[5]Space Sciences Laboratory, Berkeley, CA

Key Points:

- Direct and local comparisons between between space and laboratory plasmas of magnetic fields, current profiles, outflow jets during magnetic reconnection.
- During guide-field reconnection the energy conversion is dominated by $J_{||}E_{||}$ in both experiments.

Corresponding author: W. Fox, wfox@pppl.gov

Abstract

We present direct and scaled comparisons between laboratory and *in situ* space observations of magnetic reconnection with a guide field, comparing results from the Magnetospheric Multiscale Mission (MMS) and the Magnetic Reconnection eXperiment (MRX). While MMS observations obtains high-resolution and fully-kinetic data, MRX observations fully cover the 2-D reconnection plane near the current sheet, removing uncertainties in situating the measurements compared to the reconnection region. Through scaling transformations, we show a quantitative agreement in magnetic field and current density profiles, which agree within a factor of two from each other. The introduction of the guide field causes the energy conversion $\mathbf{J} \cdot \mathbf{E}$ in the current sheet to be dominated by $J_{||}E_{||}$ in both cases. However, parallel electric fields reported by recent spacecraft crossings are significantly (5–10x) larger than values obtained on MRX, highlighting an important issue for understanding energy conversion by reconnection.

1 Introduction

Magnetic reconnection is a fundamental process in plasmas which liberates stored magnetic energy, allowing often explosive transfer of this energy to particle flows, heat, and energized particle populations [*Yamada et al.*, 2010]. The energy conversion is mediated through current sheets, where a component of the magnetic field reverses over narrow kinetic plasma scales, accompanied by large inductive electric fields. Energy conversion by reconnection can be studied experimentally by comparing detailed measurements obtained across a number of environments, including recent *in situ* spacecraft measurements from the Magnetosphere Multiscale Mission (MMS) [*Burch et al.*, 2016], and detailed and comprehensive measurements from the Magnetic Reconnection eXperiment (MRX) [*Yamada et al.*, 1997; *Ren et al.*, 2005; *Ji et al.*, 2008; *Fox et al.*, 2017], and other laboratory experiments [*Egedal et al.*, 2007; *Fox et al.*, 2008].

In its first mission phase, MMS has observed reconnection events during a large number of current sheet crossings at the Earth's magnetopause, in a variety of regimes of guide field strength and at various distances downstream from the diffusion region. Here we focus on recent measurements of strong energy conversion processes by parallel electric fields observed during crossings close to the electron diffusion region, during guide field reconnection [*Ergun et al.*, 2016; *Eriksson et al.*, 2016; *Øieroset et al.*, 2016; *Wilder et al.*, 2017; *Phan et al.*, 2018]. The parallel electric field is important in diffusion regions, especially with a finite guide field, as it is a primary mechanism of energy conversion which directly accelerates electrons [*Kleva et al.*, 1995; *Pritchett*, 2004; *Swisdak et al.*, 2005; *Egedal et al.*, 2012]. These recent MMS events occurred in a variety of reconnection environments away from the magnetopause proper, including the turbulent region downstream of the Earth's bowshock [*Phan et al.*, 2018], in the magnetosheath [*Wilder et al.*, 2017], or embedded in Kelvin-Helmholtz vortices on the flanks of the magnetopause [*Eriksson et al.*, 2016].

Laboratory experiments such as MRX provide valuable complements to spacecraft data. The MRX experiment [*Yamada et al.*, 1997; *Ren et al.*, 2008; *Fox et al.*, 2017] enables large ensemble averages, high accuracy and spatial resolution, and comprehensive measurements over the 2-D reconnection plane (the LN plane in the standard LMN reconnection coordinate system). While MMS can obtain high resolution fully-kinetic data, the data are based on the trajectories of four spacecraft through the reconnection region, which requires assumptions to understand how given observations fit in with the global current sheet geometry, and uncertainty remains how to untangle the temporal and spatial dependence. In contrast, MRX experiments document the evolution of all quantities on the full 2-D plane in every discharge, providing a holistic picture of the reconnection events with well-characterized driving conditions and a large number of repeatable events to obtain statistics.

In this Letter we report new insights obtained through a detailed, scaled comparison of MRX and MMS data. Quantitative agreement is obtained on the magnetic field and current density structures, including the current sheet width and magnitude of the current density, and presence of electron outflow jets. Both experiments observe that energy conversion $\mathbf{J} \cdot \mathbf{E}$ becomes dominated by the $J_{||}E_{||}$ component during guide field reconnection, in contrast to the zero-guide field case where dissipation is dominated by $\mathbf{J}_\perp \cdot \mathbf{E}_\perp$ [*Yamada et al.*, 2014]. This last point of agreement is only qualitative, however, because significant differences are observed in the magnitude of the parallel and reconnection electric fields, and correspondingly the overall dissipation rates. We find on MRX that typically $E_{||} = 0.3\ V_{A,up}B_{up}$ during steady reconnection. Scaling to space plasma parameters, this value is close to or below the detection limit for MMS. However, parallel and out-of-plane electric field components significantly *above* ($\sim$ 10x) the detection limit have been reported for recent MMS events [*Burch et al.*, 2016; *Eriksson et al.*, 2016; *Wilder et al.*, 2017; *Phan et al.*, 2018]. This difference highlights a significant issue for understanding energy conversion by reconnection in space and laboratory plasmas, and we discuss several hypotheses and avenues for follow-up investigation.

2 MRX Observations

For this comparison, we use data from recent experiments on MRX studying the role of two-fluid effects during guide field reconnection [*Fox et al.*, 2017]. Through comprehensive 2D profile measurements, obtained over ~1000 reproducible discharges, these experiments observed the characteristic quadrupolar electron pressure variation and demonstrated how the parallel gradient of electron pressure balances $E_{||}$ over the ion diffusion region, an effect originally predicted in two-fluid simulations [*Aydemir*, 1992; *Wang and Bhattacharjee*, 1993; *Kleva et al.*, 1995] and particle simulations [*Ricci et al.*, 2004; *Swisdak et al.*, 2005].

Figure 1 shows a comprehensive set of 2-D profiles which serve as the basis for the comparisons below. Some of these profiles were published by *Fox et al.* [2017], but are presented in their entirety here for comparison with MMS. Quantities are plotted first in terms of physical units, but will be plotted in normalized units below when comparisons are made with MMS data. In MRX coordinates, measurements are obtained in the Z-R plane relative to the location of the x-point, where R is the radial direction in MRX which goes across the current sheet, and Z goes along the sheet. This corresponds to the L-N reconnection plane commonly used for interpreting spacecraft measurements. The conversion to LMN coordinates for MRX is based on the known magnetic geometry and does not require the maximum-variance analysis to determine the transformation. The MRX measurement area is about 16×10 cm, which corresponds to $4 \times 2.5\ \rho_s$, using the characteristic sound ion-gyroradius $\rho_s = \sqrt{T_e/m_i} \cdot (m_i/eB_{tot}) \approx 3.8$ cm.

Starting in the top left, we plot the upstream reconnecting component B_L (a), the downstream reconnected component B_N (b), and the out-of-plane component B_M (c), which consists of an overall guide field with a quadrupolar variation [*Tharp et al.*, 2012; *Fox et al.*, 2017]. Note that we have offset the color axis around the average value of -8 mT to illustrate the quadrupolar variation of B_M near the reconnection layer. The next panels show the plasma current structure near the x-point, including the out-of-plane current J_M (d), in-plane current J_L (f), which shows a strong electron-outflow-jet structure ejected to the right from the x-point, and $J_{||}$ (e). ($J_{||}$ has the opposite sign from J_M due to the negative guide field in this coordinate system.)

The top-right of the figure continues with electric field observations. The electric fields observed in MRX result from both out-of-plane, inductive electric fields E_M associated with reconnection, and in-plane components E_N and E_L. (The electric field measurement techniques are briefly reviewed in the Supplementary.) The out-of-plane component E_M is uniform within 20% over the measurement region, consistent with quasi-steady reconnection. The in-plane components E_N and E_L show much more structure and result from plasma response throughout the current sheet. $E_{||}$ is calculated from all components using the knowledge of the magnetic geometry. Like $J_{||}$, $E_{||}$ is negative due to the negative guide field in this coordinate system. The magnitude of $E_{||}$ is observed to peak at the reconnection x-point, and to decrease going away from the reconnection layer, consistent with a trend to reach an "MHD" outer region where $E_{||} \sim 0$.

Finally, magnetic field energy conversion is measured through $\mathbf{J} \cdot \mathbf{E}$, for which all vector components are measured. We directly observe that almost all dissipation is accounted through $J_{||}E_{||}$, which results because the out-of-page current J_M is dominant and co-aligns with the guide field over most of region. Previous MRX results demonstrated that at zero guide field the primary energy dissipation is $\mathbf{J}_\perp \cdot \mathbf{E}_\perp$ [*Yamada et al.*, 2014], and this comparison therefore shows that the dissipation physics shifts nearly completely to the $J_{||}E_{||}$ channel by the present guide field of $B_g/B_{up} = 0.8$. The peak dissipation occurs near the reconnection x-point and over a current layer which extends approximately 1 ρ_s downstream from the x-point in either direction. A similar trend toward dissipation dominated by $J_{||}E_{||}$ during guide-field reconnection has also been observed in recent statistical analysis of MMS events [*Wilder et al.*, 2018], electron-scale reconnection events in turbulent plasmas [*Phan et al.*, 2018], and recent particle simulations [*Pucci et al.*, 2018].

3 Comparison with MMS observations

MRX results are compared one-to-one against two recent *in situ* MMS reconnection observations [*Eriksson et al.*, 2016; *Wilder et al.*, 2017] at finite guide fields $B_g/B_{up} = 0.5$ and 4. To compare the MMS and MRX observations, we use the following scaling transformations: Magnetic fields are normalized to the upstream magnetic field B_{up}, and length scales are normalized to the ion sound gyroradius $\rho_s = \sqrt{T_{e0}/m_i} \cdot (m_i/eB_{tot})$, where $B_{tot} = (B_{up}^2 + B_g^2)^{1/2}$, and using the electron temperature in the current sheet T_{e0}. Here B_g is the out-of-plane guide magnetic field (B_M) evaluated at the reconnection layer. We convert the MMS spacecraft measurements, which are functions of time, to functions of space in the sheet-normal direction using the normal component of the ion-velocity (V_{Ni}, typically 100 km/s) averaged over the crossing, assuming that the profiles are otherwise stationary during the crossing time. Currents are then normalized to $J_0 = B_{up}/\mu_0\rho_s$, and electric fields are

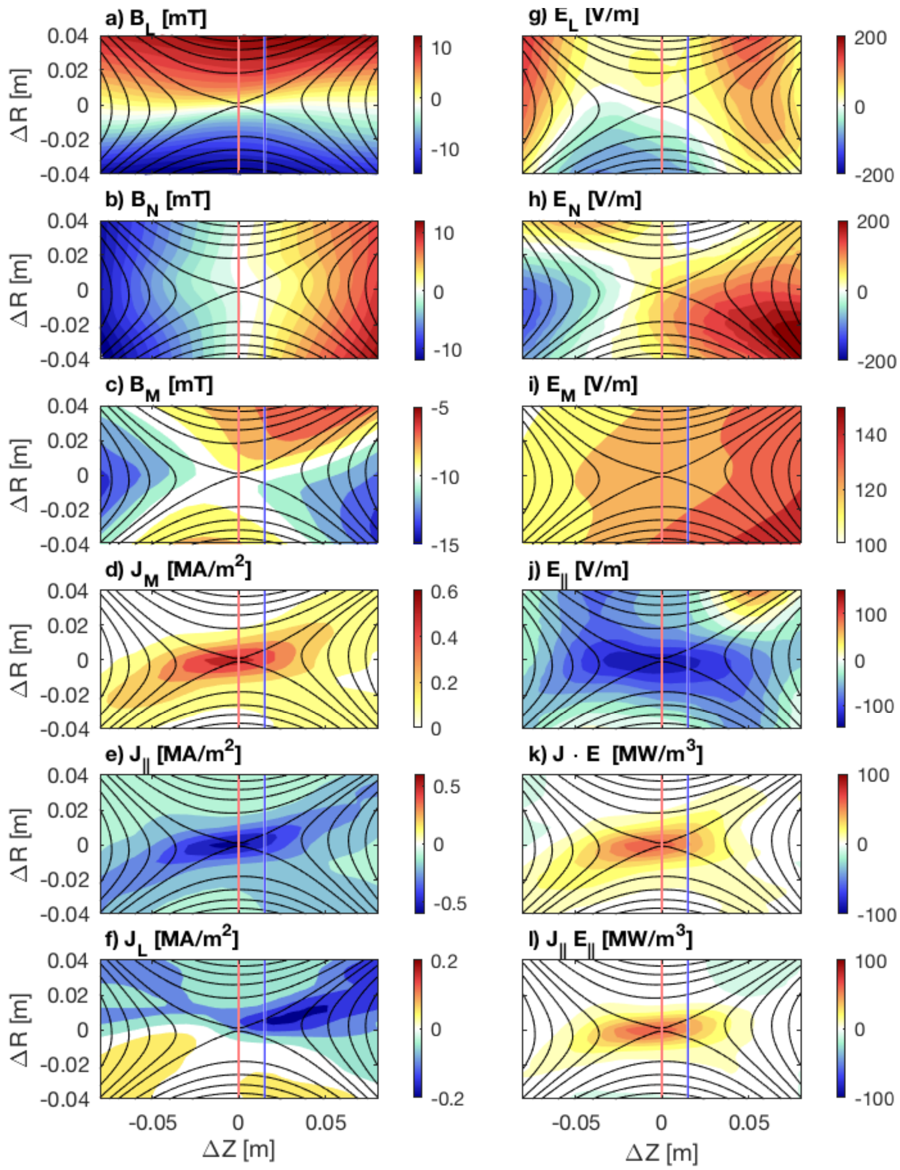

Figure 1. 2-D profiles of magnetic fields (a-c), plasma current (d-f), electric fields (g-j) and energy conversion rates (k-l) from MRX guide-field experiments. The red line and blue lines show locations of cuts across the x-line and about +0.3 ρ_s downstream which are used for comparison with MMS. See text for further descriptions of individual panels.

Table 1. Dimensional scaling parameters for comparison of laboratory and space magnetic reconnection data, and a comparison of observations in dimensionless form below

Quantity	MRX [*Fox et al.*, 2017]	MMS [*Wilder et al.*, 2017]	MMS [*Eriksson et al.*, 2016]
ions	He^+	H^+	H^+
n_0	2 10^{13} cm^{-3}	20 cm^{-3}	14 cm^{-3}
T_{e0}	8 eV	80 eV	80 eV
B_{up}	13 mT	22 nT	20 nT
B_g	8 mT	10 nT	70 nT
B_{tot}	15 mT	25 nT	75 nT
ρ_s	3.8 cm	32 km	12 km
d_i	10 cm	51 km	61 km
$V_{A,up}$	32 km/s	110 km/s	120 km/s
$E_0 = V_{A,up} B_{up}$	400 V/m	2.4 mV/m	2.4 mV/m
$J_0 = B_{up}/\mu_0 \rho_s$	0.28 MA/m^2	0.56 μA/m^2	1.3 μA/m^2
$\beta_{up} = \frac{2\mu_0 n_0 T_{e0}}{B_{up}^2}$	0.4	1.3	1.1
$\overline{E_M}$ / E_0	0.3 ± 0.1	0.15	0.2
max($E_{\|\|}$) / E_0	0.3 ± 0.1	1.5 ± 0.5	6 ± 2
max(J_M) / J_0	2 ± 0.4	3 ± 1	1.5 ± 0.3
current sheet width w/ρ_s	0.55 ± 0.1	0.3 ± .06	0.65 ± .15

normalized to the Alfvenic rate $E_0 = V_{A,up} B_{up}$, where $V_{A,up}$ is evaluated using B_{up} and the density at the x-point. Table 1 shows a summary of the scaling parameters, as well as comparison measurements in dimensionless form which are discussed below. The present MRX and MMS experiments find comparable current sheet layer widths, in units of ρ_s. This is important as it provides a basis for a comparison between these experiments. Furthermore it contributes data toward understanding the broader question of the scaling of the current sheet width, which is not yet known experimentally.

Figure 2 shows comparisons of MRX (red traces and bands) against the large guide field event of *Eriksson et al.* [2016] (blue), which had $B_g/B_{up} \sim 4$, whereas the MRX event had $B_g/B_{up} = 0.8$. Recent MRX observations has shown that the reconnection rate decreases as a function of guide field [*Tharp et al.*, 2012; *A. v. Stechow et al.*, 2018] but has largely saturated its decrease by 0.8, supporting such a comparison. In this event, MMS3

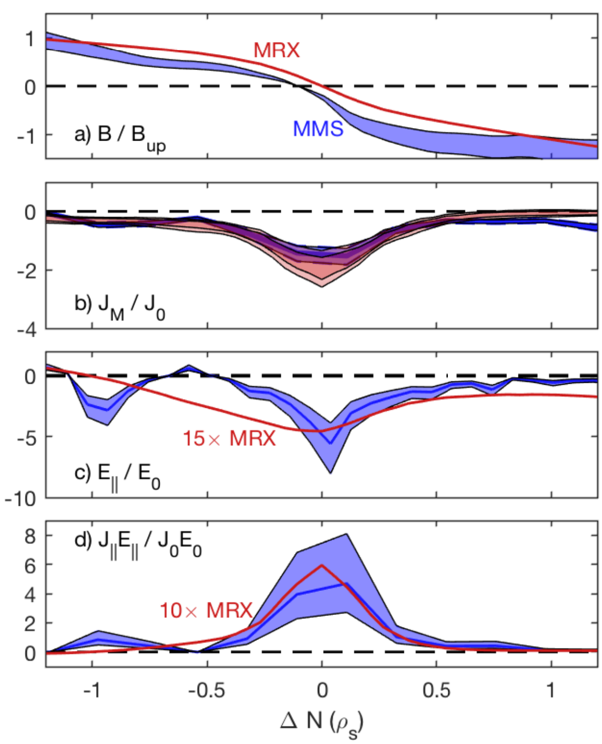

Figure 2. Scaled comparison of MRX (red curves and bands) and MMS (blue bands) data from the event of [*Eriksson et al.*, 2016], for cuts of the reconnecting magnetic field (B_L, a), current density (J_M,b), electric field ($E_{||}$,c), and energy dissipation rate ($\mathbf{J} \cdot \mathbf{E}$, d).

and MMS4 are believed to have crossed the current sheet within the electron diffusion region. Accordingly, we cut the MRX data directly across the x-point, along the red line of Fig. 1. Figure 2a compares the reconnecting components B_L, which show a good agreement of overall shape, though with a slight spatial offset (the sets are aligned based on the peak of the current density). The error bands on the MMS data in all the plots indicate a ± 20% uncertainty in defining B_{up} for the scaling transformation, which is propagated to the other quantities. Figure 2b compares the out-of-plane current J_M. Error bands on the MRX data shows range of variation at the 67% and 90% intervals over the entire data set, showing the high reproducibility of MRX. The current profile is in agreement within error bands, with the peak MMS current density about 40% lower than MRX. The current sheet widths range from 0.55-0.65ρ_s are in good agreement and coincide within error bars.

Qualitatively, both experiments observe a peak of $E_{||}$ at the x-line, which is dominated by E_M owing to the strong guide field. However, the experiments show significantly different magnitude in E_M and $E_{||}$, and therefore the energy conversion rate $\mathbf{J} \cdot \mathbf{E}$. We note that even though the *magnitudes* of $\mathbf{J} \cdot \mathbf{E}$ disagree, in both cases the dissipation is dominated by $J_{||}E_{||}$. In MRX, $E_{||} \sim 0.3V_{A,up}B_{up}$, which is approximately 1/10 the MMS value for this event. The MMS observations also show a localized spike of E_M localized near the x-point. The spike magnitude ranged from -6 mV/m $\sim\ 2.5V_{A,up}B_{up}$ when averaged over 30 ms, up to peak values of -16 mV/m at high time resolution (8196 samples/s). In contrast, in MRX E_M is fairly constant to within ~20% over the whole measurement region.

We next compare MRX results against recent MMS observations by *Wilder et al.* [2017] at a lower guide field value $B_g/B_{up}\ \sim\ 0.5$. The MMS spacecraft were believed to cross the current sheet slightly downstream of the electron diffusion region, such that a significant electron outflow jet was observed. The outflow jet was associated with a large-scale $E_{||}$ region denoted as an electron acceleration channel. Interestingly, downstream from the channel, electron holes were observed, which have been observed in previous laboratory guide-field reconnection experiments [*Fox et al.*, 2008, 2012]. MRX observes a comparable electron outflow jet, shown in Fig. 1f, where the strongest electron outflow jet propagates from the x-point toward the $+\Delta Z$ direction. The MRX jet is deflected toward the high-density separatrix which is the upper-right separatrix relative to the x-point (Fig. 1g), in agreement with these MMS observations *Wilder et al.* [2017], as well as guide-field simulations [*Pritchett*, 2004].

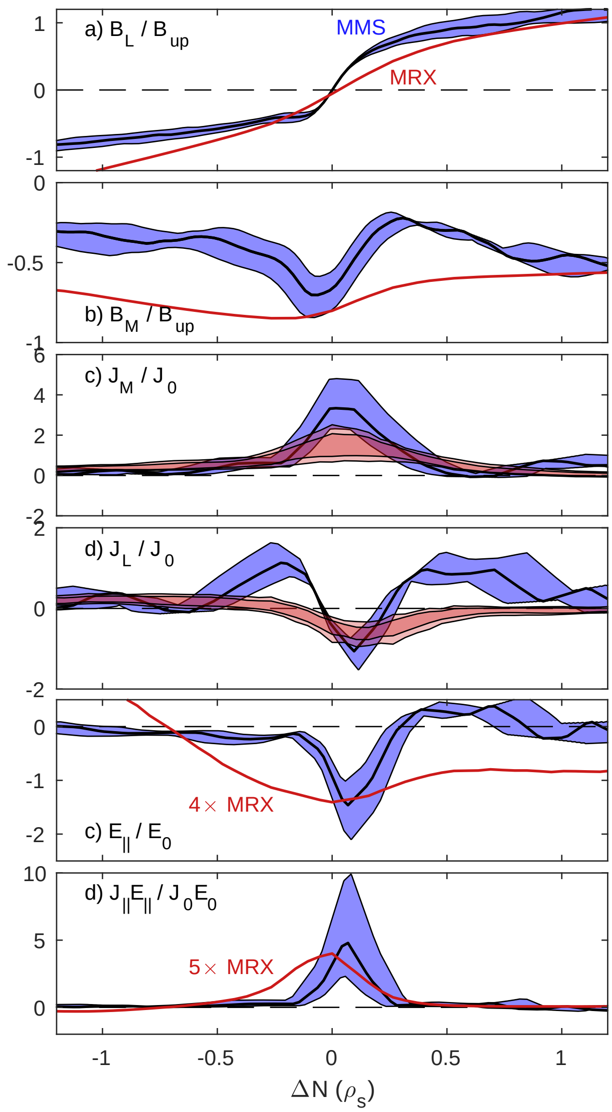

185 **Figure 3.** Scaled comparison of MRX (red curves and bands) and MMS (blue bands) data from the [*Wilder*
186 *et al.*, 2017] event, for cuts of the reconnecting magnetic field (B_L, a), out-of-plane field (B_M, b), current
187 density (J_M, c), electron outflow jet (J_L, d), electric field ($E_{||}$, e), and energy dissipation rate ($\mathbf{J} \cdot \mathbf{E}$, f).

For comparison with MRX, we take a cut a short distance ($\sim 0.3\ \rho_s$) downstream of the x-point (Fig. 1, blue trace), which crosses both the peak out-of-plane current (J_M) and the beginning of the outflow jet (J_L). Figure 3 shows the detailed one-to-one comparison along these cuts. The overall current sheet width over which the magnetic field reverses (B_L, Fig. 3a), and the associated current density (J_M, c), are in reasonable agreement, though we observe that the MMS current sheet is "sharper" by about a factor of 2, resulting in a narrower current sheet and stronger current density. The MMS observations show a larger and sharper variation of B_M and the associated outflow-jet current J_L. The MMS traces also show a pronounced "return" current ($J_L > 0$) on either side of the jet ($J_L < 0$) which is not apparent in the present MRX data in the guide field regime, though has been observed previously at zero guide field [*Ren et al.*, 2008]. Finally, as before $E_{||}$ and dissipation are compared, and indicate significantly larger $E_{||}$ and $\mathbf{J} \cdot \mathbf{E}$ on MMS than MRX. In this case, the peak $E_{||}$ for MMS is 1–2 $V_{A,up} B_{up}$, a factor 3–5 above the MRX values.

To help understand these large local MMS electric fields, we also estimate and compare a "global" reconnection electric field $\overline{E_M}$ for these MMS crossings based on consideration of inflow of magnetic flux by plasma flow into the sheet. On longer timescales (several ω_{ci}^{-1}) one expects that the reconnection of flux (corresponding to $\overline{E_M}$) balances the inflow of flux into the layer ($V_{in} \times B_{up}$). This balance is routinely confirmed on MRX; for MMS, by examining averaged inflows for several ω_{ci}^{-1} upstream on either side, an estimate can be made of $V_{in} \times B_{up}$ over a larger scale than just the current sheet. The *Wilder et al.* [2017] results show an ion inflow reversal of $V_{in} \sim \Delta V_{Ni}/2 \sim 20$ km/s across the sheet, and an upstream field B_{up} ~20 nT, which imply a global $\overline{E_M} \sim V_{in} B_{up} \sim 0.4$ mV/m ~ $0.15 V_{A,up} B_{up}$. While this is a somewhat crude estimate, it is worth noting that this value is much smaller than the peak E_M and $E_{||}$ observed in the reconnection layer, and much more in line with the MRX values for E_M and $E_{||}$. A comparable estimate is also possible for the event of *Eriksson et al.* [2016], again finding upstream $V_{in} \times B_{up}$ much smaller than the peak $E_{||}$ and E_M (Table 1). We conclude that "global" reconnection rates $\overline{E_M}$ are in agreement between MRX and MMS, but that MMS can observe a significant enhancement of $E_{||}$ and E_M in the reconnection layer itself.

Finally, in comparing electric fields, it is important to pay attention to commensurate measurement timescales for the two experiments. In general, MMS spacecraft traverse reconnection current sheets very quickly based on the fast relative speed of the plasma and spacecraft and so make "snapshot" measurements of the current sheet. In the events reported by *Wilder et al.* [2017], the large $E_{||}$ structures were observed on all 4 MMS spacecraft, implying these structures persisted for at least $\tau_{\mathrm{MMS}} \gtrsim 0.2$ s [*Wilder et al.*, 2017], which corresponds to $\gtrsim 0.4\omega_{ci}^{-1}$ in scaled ion units. The events observed by *Eriksson et al.* [2016] similarly were observed by two spacecraft separated by 0.4 s. To achieve a comparable time resolution for MRX, we modified the MRX analysis pipeline to decrease the software time-filtering. Notably, changing the bandwidth did not change the observed E_M values $\sim 0.3\ B_{up}V_{A,up}$ significantly: the magnitudes were still far different from the large $E_{||}$ and E_M fields observed by MMS, nor were any outliers obtained over 300 analyzed discharges that reached the MMS values. The resulting averaging time, including the finite bandwidth of the coils and digitizers, is $\tau_{MRX} = 2.2\ \mu$s $= 0.75\ \omega_{ci}^{-1}$, which is within a factor of 2 of the MMS "measurement time." We conclude it is a significant difference in plasma physics between the systems that leads to the different observations of E_M and $E_{||}$, rather than a measurement effect.

4 Discussion and Outlook

This Letter has presented scaled one-to-one comparisons of laboratory and spacecraft observations of guide-field magnetic reconnection. A set of scaling laws was presented, which allows the two experiments to be compared despite 12 orders of magnitude difference in density, and 6 orders of magnitude in magnetic fields. The basic agreement results from the current sheet thinning to close to the ion scale in both systems, to approximately 0.5 ρ_s. Quantities such as the width of the current sheet and magnitude of the current density are within a factor of two agreement between MRX and both MMS events analyzed. The experiments demonstrate the dominance of reconnection dissipation by $J_{||}E_{||}$ during guide field reconnection. Both experiments find current sheets slightly below the ρ_s scale. This provides valuable data toward understanding the scaling of the current sheet width with plasma parameters, which is an important constraint for reconnection models [*Ji et al.*, 2008]. However, the identification of other events with widths as low as 0.1 ρ_s (in non-ion-coupled regimes by *Phan et al.* [2018]) argues that broader data is warranted. Future analysis utilizing more events (for MMS) or experiments over a wide range of plasma parameters (MRX) will be valuable to determine what sets the scaling for the current sheet thickness during guide field reconnection.

Extremely strong local $E_{||}$ and E_M, up to ~5 $V_{A,up}B_{up}$, coincident with the reconnection crossing have been documented in several MMS crossing events including those compared here. In contrast, MRX generally observes much smaller $E_{||}$ and $E_M = 0.3\ V_{A,up} B_{up}$, which however appear consistent with estimates for the "global" reconnection rates by MMS. These differences raise significant questions for understanding these strong electric fields during reconnection, whether they are transient or steady, how they are driven, and what role they play in reconnection layers. Even if transient, these large electric fields could be important for the overall energy balance during reconnection, if $\langle \mathbf{J} \cdot \mathbf{E} \rangle$ is larger than $\langle \mathbf{J} \rangle \cdot \langle \mathbf{E} \rangle$, where the latter indicate the values associated with the average behavior of the current sheet. We now explore some possible hypotheses for these different observations.

We first note the possible effect of residual plasma parameter differences between the systems. The plasma β in MRX is smaller by a factor of ~ 3. In the event where the outflow jet could be compared [*Wilder et al.*, 2017], the guide field in MRX is stronger by a factor of 2. This may explain the difference in the jet structure observed: by pressure balance, the variation in the scaled Hall field $\delta B_M / B_{up}$ should scale like $\beta_{up} \times (B_{up}/B_g)$, which indicates that at lower pressure and at stronger guide field, the jets should become weaker, which is the correct trend. However, it is not known how the plasma β would affect the electric fields. A second difference is that MRX is at a finite collisionality, with the electron mean-free-path of order 10 cm $\sim 2\rho_s$. However, the collisionality is sufficiently low so that the collisional resistivity does not play a role in determining the reconnection electric field in Ohm's law, $E_M \gg \eta J_M$, and for this reason it is not clear how this difference would explain the very significant differences in observed E_M or $E_{||}$.

A second hypothesis to explain the large observed electric fields and energy conversion is that MMS is observing a transient or bursty reconnection driven by large-scale waves or the dynamics of flux ropes or plasmoids in the current sheet. The present MRX observations were obtained in a well-controlled and steady regime [*Fox et al.*, 2017] (to obtain clean measurements of the structure of guide-field current sheets), and unfortunately this limits the ability to make predictions of non-steady reconnection dynamics with a guide field. However, previous MRX observations at zero-guide-field have observed non-steady, impulsive reconnection, resulting from sudden current sheet disruptions and flux rope ejection [*Dorfman et al.*, 2013]. These non-steady current dynamics drove a strong time-dependence of the magnetic field and enhanced peak reconnection rates up to $E_M \sim 1 V_{A,up} B_{up}$. Notably the disruption occurred on a timescale $\tau \sim 3\ \mu$s = 2-3 ω_{ci}^{-1} which could still appear quasi-constant during a spacecraft crossing. (e.g. $\tau \sim 0.4\omega_{ci}^{-1}$ for *Wilder et al.* [2017]). Reconnection events driven by KH waves in the magnetopause flank have been proposed to contain multiple flux ropes which might support such dynamics [*Eriksson et al.*, 2009; *Nakamura et al.*, 2017; *Sturner et al.*, 2018]. Recent observations in sub-ion scale current sheets have also observed very large parallel electric fields $E_{||} \sim 5E_0$ [*Phan et al.*, 2018]; this presents a second idea that large reconnection rates may be linked to reconnection at small spatial scales. Future experiments at MRX will be valuable to study the structure and magnitude of $E_{||}$ and E_M during impulsive guide-field reconnection events and at various scale sizes, for comparison against these MMS results.

To conclude, these results provide a scaled one-to-one comparison between laboratory and space plasmas undergoing guide field magnetic reconnection. Beyond showing a basic agreement, this first quantitative comparison raises interesting questions for future work, including understanding the scaling of the current sheet with plasma parameters, the magnitude and structure of outflow jets, and the nature of large electric fields observed by MMS. While this work has focused on a physics comparison between *experiments*, particle simulations will undoubtably provide insights into the issues identified here.

Acknowledgments

This work was supported by the Max-Planck Princeton Center for Plasma Physics, funded by the U.S. Department of Energy under Contract No. DE-AC0204CH11466 and NASA under Agreements No. NNH15AB29I and No. NNH14AX631. MRX digital data is available from http://arks.princeton.edu/ark:/88435/dsp01x920g025r. MMS data is available from the MMS Science Data Center.

References

A. v. Stechow, W. Fox, J. Jara-Almonte, J. Yoo, H. Ji, and M. Yamada (2018), Electromagnetic fluctuations during guide field reconnection in a laboratory plasma, *Phys. Plasmas*, *25*(5), 052,120, doi:10.1063/1.5025827.

Aydemir, A. Y. (1992), Nonlinear studies of m=1 modes in high-temperature plasmas, *Phys. Fluids B: Plasma Phys. (1989-1993)*, *4*(11), 3469–3472, doi:10.1063/1.860355.

Burch, J. L., R. B. Torbert, T. D. Phan, L. J. Chen, T. E. Moore, R. E. Ergun, J. P. Eastwood, D. J. Gershman, P. A. Cassak, M. R. Argall, S. Wang, M. Hesse, C. J. Pollock, B. L. Giles, R. Nakamura, B. H. Mauk, S. A. Fuselier, C. T. Russell, R. J. Strangeway, J. F. Drake, M. A. Shay, Y. Khotyaintsev, P. A. Lindqvist, G. Marklund, F. D. Wilder,

D. T. Young, K. Torkar, J. Goldstein, J. C. Dorelli, L. A. Avanov, M. Oka, D. N. Baker, A. N. Jaynes, K. A. Goodrich, I. J. Cohen, D. L. Turner, J. F. Fennell, J. B. Blake, J. Clemmons, M. Goldman, D. Newman, S. M. Petrinec, K. J. Trattner, B. Lavraud, P. H. Reiff, W. Baumjohann, W. Magnes, M. Steller, W. Lewis, Y. Saito, V. Coffey, and M. Chandler (2016), Electron-scale measurements of magnetic reconnection in space, *Science*, *352*(6290), aaf2939.

Dorfman, S., H. Ji, M. Yamada, J. Yoo, E. Lawrence, C. Myers, and T. D. Tharp (2013), Three-dimensional, impulsive magnetic reconnection in a laboratory plasma, *Geophys. Res. Lett.*, *40*(2), 233–238, doi:10.1029/2012gl054574.

Egedal, J., W. Fox, N. Katz, M. Porkolab, K. Reim, and E. Zhang (2007), Laboratory Observations of Spontaneous Magnetic Reconnection, *Phys. Rev. Lett.*, *98*(1), 015,003.

Egedal, J., W. Daughton, and A. Le (2012), Large-scale electron acceleration by parallel electric fields during magnetic reconnection, *Nature Phys.*, *8*(4), 321–324.

Ergun, R. . E., K. . A. Goodrich, F. . D. Wilder, J. . C. Holmes, J. . E. Stawarz, S. Eriksson, A. . P. Sturner, D. . M. Malaspina, M. . E. Usanova, R. . B. Torbert, P. A. Lindqvist, Y. Khotyaintsev, J. . L. Burch, R. . J. Strangeway, C. . T. Russell, C. . J. Pollock, B. . L. Giles, M. Hesse, L. . J. Chen, G. Lapenta, M. . V. Goldman, D. . L. Newman, S. . J. Schwartz, J. . P. Eastwood, T. . D. Phan, F. . S. Mozer, J. Drake, M. . A. Shay, P. . A. Cassak, R. Nakamura, and G. Marklund (2016), Magnetospheric Multiscale Satellites Observations of Parallel Electric Fields Associated with Magnetic Reconnection, *Phys. Rev. Lett. 116*(23), 235102.

Eriksson, S., H. Hasegawa, W. L. Teh, B. U. O. Sonnerup, J. P. McFadden, K. H. Glassmeier, O. Le Contel, V. Angelopoulos, C. M. Cully, D. E. Larson, R. E. Ergun, A. Roux, and C. W. Carlson (2009), Magnetic island formation between large-scale flow vortices at an undulating postnoon magnetopause for northward interplanetary magnetic field, *J. Geophys. Res.*, *114*, A00C17.

Eriksson, S., F. D. Wilder, R. E. Ergun, S. J. Schwartz, P. A. Cassak, J. L. Burch, L. J. Chen, R. B. Torbert, T. D. Phan, B. Lavraud, K. A. Goodrich, J. C. Holmes, J. E. Stawarz, A. P. Sturner, D. M. Malaspina, M. E. Usanova, K. J. Trattner, R. J. Strangeway, C. T. Russell, C. J. Pollock, B. L. Giles, M. Hesse, P. A. Lindqvist, J. F. Drake, M. A. Shay, R. Nakamura, and G. T. Marklund (2016), Magnetospheric Multiscale Observations of the Electron Diffusion Region of Large Guide Field Magnetic Reconnection, *Phys. Rev. Lett.*, *117*, 015001.

Fox, W., M. Porkolab, J. Egedal, N. Katz, and A. Le (2008), Laboratory Observation of Electron Phase-Space Holes during Magnetic Reconnection, *Phys. Rev. Lett.*, *101*(25), 255003.

Fox, W., M. Porkolab, J. Egedal, N. Katz, and A. Le (2012), Observations of electron phase-space holes driven during magnetic reconnection in a laboratory plasma, *Phys. Plasmas*, *19*(3), 032118.

Fox, W., F. Sciortino, A. v. Stechow, J. Jara-Almonte, J. Yoo, H. Ji, and M. Yamada (2017), Experimental Verification of the Role of Electron Pressure in Fast Magnetic Reconnection with a Guide Field, *Phys. Rev. Letters*, *118*(12), 125002.

Ji, H., Y. Ren, M. Yamada, S. Dorfman, W. Daughton, and S. P. Gerhardt (2008), New insights into dissipation in the electron layer during magnetic reconnection, *Geophys. Res. Lett.*, *35*(13), L13,106.

Kleva, R. G., J. F. Drake, and F. L. Waelbroeck (1995), Fast reconnection in high temperature plasmas, *Phys. Plasmas* , *2*(1), 23.

Nakamura, T. K. M., H. Hasegawa, W. Daughton, S. Eriksson, W. Y. Li, and R. Nakamura (2017), Turbulent mass transfer caused by vortex induced reconnection in collisionless magnetospheric plasmas, *Nature Comm.*, *8*(1).

Øieroset, M., T. D. Phan, C. Haggerty, M. A. Shay, J. P. Eastwood, D. J. Gershman, J. F. Drake, M. Fujimoto, R. E. Ergun, F. S. Mozer, M. Oka, R. B. Torbert, J. L. Burch, S. Wang, L. J. Chen, M. Swisdak, C. Pollock, J. C. Dorelli, S. A. Fuselier, B. Lavraud, B. L. Giles, T. E. Moore, Y. Saito, L. A. Avanov, W. Paterson, R. J. Strangeway, C. T. Russell, Y. Khotyaintsev, P. A. Lindqvist, and K. Malakit (2016), MMS observations of large guide field symmetric reconnection between colliding reconnection jets at the center of a magnetic flux rope at the magnetopause, *Geophys. Res. Lett.*, *43*(11), 5536–5544.

Phan, T. D., J. P. Eastwood, M. A. Shay, J. F. Drake, B. U. O. Sonnerup, M. Fujimoto, P. A. Cassak, M. Øieroset, J. L. Burch, R. B. Torbert, A. C. Rager, J. C. Dorelli, D. J. Gershman, C. Pollock, P. S. Pyakurel, C. C. Haggerty, Y. Khotyaintsev, B. Lavraud, Y. Saito, M. Oka, R. E. Ergun, A. Retino, O. Le Contel, M. R. Argall, B. L. Giles, T. E. Moore, F. D. Wilder, R. J. Strangeway, C. T. Russell, P. A. Lindqvist, and W. Magnes (2018), Electron magnetic reconnection without ion coupling in Earth's turbulent magnetosheath, *Nature*, *557*(7704).

Pritchett, P. L. (2004), Three-dimensional collisionless magnetic reconnection in the presence of a guide field, *J. Geophys. Res.*, *109*(A1), A01220.

Pucci, F., S.Usami, H. Ji, X. Guo, R. Horiuchi, S. Okamura, W. Fox, J. Jara-Almonte, M. Yamada, , and J. Yoo (2018), Energy transfer and electron energization in collisionless magnetic reconnection for different guide-field intensities, *submitted to Phys. Plasmas*.

Ren, Y., M. Yamada, S. Gerhardt, H. Ji, R. Kulsrud, and A. Kuritsyn (2005), Experimental verification of the Hall effect during magnetic reconnection in a laboratory plasma, *Phys. Rev. Lett.*, *95*(5), 055003.

Ren, Y., M. Yamada, H. Ji, S. P. Gerhardt, and R. Kulsrud (2008), Identification of the Electron-Diffusion Region during Magnetic Reconnection in a Laboratory Plasma, *Phys. Rev. Lett.*, *101*(8).

Ricci, P., J. U. Brackbill, W. Daughton, and G. Lapenta (2004), Collisionless magnetic reconnection in the presence of a guide field, *Phys. Plasmas*, *11*(8), 4102–4114.

Sturner, A. P., S. Eriksson, T. Nakamura, D. J. Gershman, F. Plaschke, R. E. Ergun, F. D. Wilder, B. Giles, C. Pollock, W. R. Paterson, R. J. Strangeway, W. Baumjohann, and J. L. Burch (2018), On Multiple Hall-Like Electron Currents and Tripolar Guide Magnetic Field Perturbations During Kelvin-Helmholtz Waves, *J. Geophys. Res.*, *123*(2), 1305.

Swisdak, M., J. F. Drake, and M. A. Shay (2005), Transition from antiparallel to component magnetic reconnection, *J Geophys. Res.*, *110*(A5).

Tharp, T. D., M. Yamada, H. Ji, E. Lawrence, S. Dorfman, C. E. Myers, and J. Yoo (2012), Quantitative Study of Guide-Field Effects on Hall Reconnection in a Laboratory Plasma, *Phys. Rev. Lett.*, *109*, 165002.

Wang, X., and A. Bhattacharjee (1993), Nonlinear dynamics of the $m = 1$ instability and fast sawtooth collapse in high-temperature plasmas, *Phys. Rev. Lett.*, *70*, 1627.

Wang, X., A. Bhattacharjee, and Z. W. Ma (2000), Collisionless reconnection: Effects of Hall current and electron pressure gradient, *J. Geophys. Res.*, *105*(A12), 27,633–27,648.

Wilder, F. D., R. E. Ergun, S. Eriksson, T. . D. Phan, J. . L. Burch, N. Ahmadi, K. . A. Goodrich, D. . L. Newman, K. . J. Trattner, R. . B. Torbert, B. . L. Giles, R. J. Strangeway, W. Magnes, P. A. Lindqvist, and Y.-V. Khotyaintsev (2017), Multipoint Measurements of the Electron Jet of Symmetric Magnetic Reconnection with a Moderate Guide Field, *Phys. Rev. Lett.*, *118*(26).

Wilder, F. D., R. E. Ergun, J. L. Burch, N. Ahmadi, S. Eriksson, T. D. Phan, K. A. Goodrich, J. Shuster, A. C. Rager, R. B. Torbert, B. L. Giles, R. J. Strangeway, F. Plaschke, W. Magnes, P. A. Lindqvist, and Y. V. Khotyaintsev (2018), The role of the parallel electric field in electron-scale dissipation at reconnecting currents in the magnetosheath, *J.*

Geophys. Res..

Yamada, M., H. Ji, S. Hsu, T. Carter, R. Kulsrud, N. Bretz, F. Jobes, Y. Ono, and F. Perkins (1997), Study of driven magnetic reconnection in a laboratory plasma, *Phys. Plasmas* , *4*(5).

Yamada, M., R. Kulsrud, and H. Ji (2010), Magnetic reconnection, *Rev. Mod. Phys.*, *82*(1), 603.

Yamada, M., J. Yoo, J. Jara-Almonte, H. Ji, R. M. Kulsrud, and C. E. Myers (2014), Conversion of magnetic energy in the magnetic reconnection layer of a laboratory plasma, *Nature Comm.*, *5*(1).